

A Fault Model with Two Asperities of Different Areas and Strengths

Emanuele Lorenzano¹  · Michele Dragoni¹ 

Received: 25 October 2017 / Accepted: 16 March 2018 / Published online: 9 April 2018
© International Association for Mathematical Geosciences 2018

Abstract A fault with two asperities with different areas and strengths is considered. The fault is treated as a dynamical system with two state variables (the slip deficits of the asperities) and four dynamic modes, for which complete analytical solutions are provided. The seismic events generated by the fault can be discriminated in terms of a variable related with the difference between the slip deficits of the asperities at the beginning of the interseismic interval preceding the event. The effect of the difference between the asperity areas on several features of the model, such as the force rates on the asperities, the slip duration and amplitude, the occurrence of events involving the simultaneous motion of the asperities and the radiation of elastic waves, is discussed. As an application, the M_w 8.0 2007 Pisco, Peru, earthquake is considered: it is modelled as a two-mode event due to the consecutive failure of two asperities, one almost twice as large as the other. The source function and final seismic moment predicted by the model are found to be in good agreement with observations.

Keywords Fault model · Asperity model · Asperity size · 2007 Pisco earthquake

1 Introduction

In the framework of fault dynamics, a significant complication arises from the heterogeneity of fault surfaces, which usually exhibit a strongly nonuniform friction

✉ Emanuele Lorenzano
emanuele.lorenzano2@unibo.it
Michele Dragoni
michele.dragoni@unibo.it

¹ Dipartimento di Fisica e Astronomia, Alma Mater Studiorum Università di Bologna, Viale Carlo Berti Pichat 8, 40127 Bologna, Italy

distribution. Such a distribution can be represented in terms of asperity models, assuming that earthquakes result from the failure of a small number of patches characterized by high static friction and velocity-weakening dynamic friction, while the rest of the fault gives a negligible contribution (Lay et al. 1982; Ruff 1983; Scholz 1990). Velocity-weakening (VW) is the behaviour of a fault patch characterized by a friction that decreases with increasing slip rate. Velocity-strengthening (VS) is the opposite behaviour, with friction increasing with increasing slip rate. In the framework of asperity models, fault dynamics coincides with the dynamics of the asperities and the state of the fault is described by the variables characterizing the asperities.

In this framework, discrete fault models have proved to be valuable tools to investigate fault dynamics (Ruff 1992; Rice 1993; Turcotte 1997). Such models assume that each asperity is a compact and simply connected subset of the fault surface. Asperities may have any geometrical shape and their failure can reproduce any kind of source mechanism. Since asperities are treated as single units of the fault, details of friction, stress and slip distribution on asperities are not investigated; instead, only the average values of these quantities are considered. At a given instant in time, an asperity can be either sticking or slipping. A uniform slip is assumed to take place when an asperity moves, so that asperity motions are treated as Volterra dislocations.

A manifestation of fault heterogeneity is also the presence of VW and VS regions on the same fault. This aspect has been the subject of several studies, mainly in the framework of continuous models. Chen and Lapusta (2009) considered a small fault patch governed by steady-state VW friction surrounded by a larger VS region and studied the interaction between the two regions. Skarbak et al. (2012) found that the relative proportions of VW and VS areas control the sliding character (stable, slow, or dynamic) of the fault. Luo and Ampuero (2017) found that slip of the VS region controls the stability of VW asperities, which may fail alone or involve the whole fault, including the VS region. In the present paper, we do not consider the presence of these two types of mechanical behaviour: it has been studied in the framework of a discrete fault model by Dragoni and Lorenzano (2017), who showed that the fault dynamics is characterized by three interacting slipping modes, namely stable creep, seismic slip and afterslip.

Early discrete fault models with two asperities were proposed by Nussbaum and Ruina (1987), Huang and Turcotte (1990), McCloskey and Bean (1992) and Turcotte (1997). Such models were further developed by Dragoni and Santini (2012, 2014). Wave radiation was introduced by Dragoni and Santini (2015) and Dragoni and Tallarico (2016). The evolution of the fault during interseismic intervals has been considered by Amendola and Dragoni (2013), Dragoni and Lorenzano (2015) and Dragoni and Piombo (2015).

These models assumed equal areas for the two asperities. This is a reasonable approximation in many cases, because the asperities giving a relevant contribution to an earthquake must have comparable areas. In fact, if an asperity has a much smaller area than the other one, its slip will be comparatively smaller, so that its contribution to the seismic moment will be negligible.

However, asperities with areas differing by a factor of 2 or 3 are sometimes observed (for instance, in the case of the 1964 Alaska earthquake) and taking this difference into account is a necessary refinement of previous models. In the present paper, the

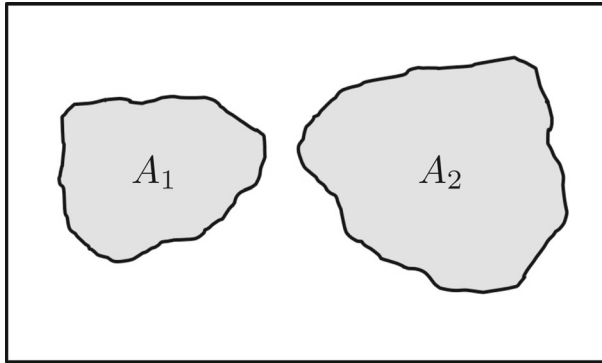


Fig. 1 The model: a fault with two asperities of areas A_1 and A_2 , respectively. The fault boundary is identified by the rectangular frame

dynamical equations of the system in the case of different areas and strengths of the asperities are presented and their solutions are calculated analytically.

As an application of the model, the M_w 8.0 2007 Pisco, Peru, earthquake is considered. This event was ascribed to the consecutive failures of two asperities having significantly different areas.

2 The Model

A plane fault embedded in a shear zone placed between two tectonic plates moving at constant relative velocity v is considered. The shear zone is assumed to be a homogeneous and isotropic Hooke solid with rigidity μ , and the fault is subject to a shear strain rate $\dot{\epsilon}$. The fault contains two asperities (named 1 and 2) with areas A_1 and A_2 respectively (Fig. 1). Let

$$\xi = \frac{A_2}{A_1}, \tag{1}$$

and let a be the distance between the centroids of the asperities, where each centroid is defined as the integral of the positions of all the points enclosed by the given asperity. At any time t , each asperity can be characterized by its slip deficit, that is, the slip that the asperity should undergo in order to recover the relative plate displacement occurred up to time t . The state of the fault is described by the slip deficits $x(t)$ and $y(t)$ of asperity 1 and asperity 2, respectively.

Asperities move as rigid surfaces: accordingly, their dynamics can be more easily described using forces instead of tractions. The asperity motion is controlled by friction and by the forces that are exerted by the surrounding medium. Let f_1 and f_2 be the tangential forces applied to the asperities in the slip direction. They can be written as

$$f_1 = -K_1x + K_c(y - x) - t_1\dot{x}, \tag{2}$$

$$f_2 = -K_2y - K_c(y - x) - t_2\dot{y}. \tag{3}$$

In these expressions, the terms $-K_1x$ and $-K_2y$ represent the effect of tectonic loading, whereas the terms $\pm K_c (y - x)$ are the contributions of stress transfer between the asperities. The coupling constants K_1 , K_2 and K_c are given by

$$K_1 = \frac{2\mu\dot{\epsilon}A_1}{v}, \quad K_2 = \frac{2\mu\dot{\epsilon}A_2}{v}, \tag{4}$$

$$K_c = \mu A_1 A_2 s, \tag{5}$$

where s is the shear traction (per unit seismic moment) that the slip of one asperity imposes to the other, calculated at the centroid of the asperity. The terms $-\iota_1\dot{x}$ and $-\iota_2\dot{y}$ are forces due to radiation damping, where ι_1 and ι_2 are impedances (Rice 1993). Assuming that the impedance per unit area is the same for both asperities, it results

$$\frac{\iota_2}{\iota_1} = \xi. \tag{6}$$

As for friction, it is assumed that asperities 1 and 2 are characterized respectively by constant static frictions f_{s1} and f_{s2} and by average dynamic frictions f_{d1} and f_{d2} . Accordingly, the conditions for the failure of asperity 1 and 2 are, respectively

$$f_1 = -f_{s1}, \quad f_2 = -f_{s2}. \tag{7}$$

If β is the ratio between the frictional stresses of the asperities, the ratio between frictional forces is

$$\frac{f_{s2}}{f_{s1}} = \frac{f_{d2}}{f_{d1}} = \beta\xi. \tag{8}$$

Without loss of generality, it can be assumed $0 < \beta \leq 1$. Finally, it is assumed that dynamic frictions are smaller than static frictions by a factor ϵ that is the same for both asperities, that is

$$\epsilon = \frac{f_{d1}}{f_{s1}} = \frac{f_{d2}}{f_{s2}}, \tag{9}$$

with $0 < \epsilon < 1$.

To sum up, the equations of motion for the two asperities are

$$\mu_1\ddot{x} + \iota_1\dot{x} + (K_1 + K_c)x - K_cy - f_{d1} = 0, \tag{10}$$

$$\mu_2\ddot{y} + \iota_2\dot{y} + (K_2 + K_c)y - K_cx - f_{d2} = 0, \tag{11}$$

where μ_1 and μ_2 are the masses associated with the asperities, which are assumed to be proportional to the respective areas, that is

$$\frac{\mu_2}{\mu_1} = \xi. \tag{12}$$

The nondimensional variables and time

$$X = \frac{K_1x}{f_{s1}}, \quad Y = \frac{K_1y}{f_{s1}}, \quad T = \sqrt{\frac{K_1}{\mu_1}} t, \tag{13}$$

and the additional nondimensional parameters

$$\alpha = \frac{K_c}{K_1} = \frac{A_2 v s}{2 \dot{e}}, \quad \gamma = \frac{\iota_1}{\sqrt{K_1 \mu_1}}, \quad V = \frac{\sqrt{K_1 \mu_1}}{f_{s1}} v, \tag{14}$$

are introduced, with $\alpha \geq 0, \gamma \geq 0, V > 0$. Also, the nondimensional forces

$$F_1 = \frac{f_1}{f_{s1}}, \quad F_2 = \frac{f_2}{f_{s1}}, \tag{15}$$

are defined. From (2) and (3), it results

$$F_1 = -(1 + \alpha)X + \alpha Y - \gamma \dot{X}, \quad F_2 = -(\xi + \alpha)Y + \alpha X - \gamma \xi \dot{Y}, \tag{16}$$

where dots indicate differentiation with respect to T . Finally, the equations of motion (10) and (11) can be written in nondimensional form as

$$\ddot{X} + \gamma \dot{X} + (1 + \alpha)X - \alpha Y - \epsilon = 0, \tag{17}$$

$$\ddot{Y} + \gamma \dot{Y} + (1 + \alpha')Y - \alpha' X - \beta \epsilon = 0, \tag{18}$$

where the parameter

$$\alpha' = \frac{\alpha}{\xi}, \tag{19}$$

was introduced.

If the state of the fault is represented by a point of the plane XY , the points corresponding to stationary asperities belong to a subset \mathbf{Q} of the plane XY : this subset is called the sticking region (Di Bernardo et al. 2008). It can be determined as follows.

In the sticking mode, the forces (16) reduce to

$$F_1 = -(1 + \alpha)X + \alpha Y, \quad F_2 = -(\xi + \alpha)Y + \alpha X. \tag{20}$$

In nondimensional form, the conditions (7) for the failure of asperities 1 and 2 can be written as

$$F_1 = -1, \quad F_2 = -\beta \xi, \tag{21}$$

where (8) was taken into account. If overshooting is excluded, the forces must be always negative. Therefore, \mathbf{Q} includes the states of the fault in which the forces satisfy the conditions

$$-1 < F_1 \leq 0, \quad -\beta \xi < F_2 \leq 0. \tag{22}$$

Thanks to (20), conditions (21) yield the equations of the lines

$$Y = \frac{1 + \alpha}{\alpha} X - \frac{1}{\alpha}, \tag{23}$$

$$Y = \frac{\alpha}{\alpha + \xi} X + \frac{\beta \xi}{\alpha + \xi}, \tag{24}$$

called Line 1 and Line 2, respectively. The further conditions

$$F_1 = 0, \quad F_2 = 0, \quad (25)$$

yield the equations of the lines

$$Y = \frac{1 + \alpha}{\alpha} X, \quad Y = \frac{\alpha}{\alpha + \xi} X. \quad (26)$$

Let P_a be the intersection of line $F_2 = 0$ with Line 1 and P_b be the intersection of line $F_1 = 0$ with Line 2. The coordinates of points P_a and P_b are

$$X_a = \frac{\alpha + \xi}{\alpha + \alpha\xi + \xi}, \quad Y_a = \frac{\alpha}{\alpha + \alpha\xi + \xi}, \quad (27)$$

$$X_b = \frac{\alpha\beta\xi}{\alpha + \alpha\xi + \xi}, \quad Y_b = \frac{(1 + \alpha)\beta\xi}{\alpha + \alpha\xi + \xi}. \quad (28)$$

The coordinates of point P , where Lines 1 and 2 meet, are

$$X_P = X_a + X_b, \quad Y_P = Y_a + Y_b. \quad (29)$$

The sticking region \mathbf{Q} of the system is then the parallelogram enclosed by the four lines, with vertices at the origin, P_a , P_b and P (Fig. 2). Its area is

$$A_{\mathbf{Q}} = \frac{\beta\xi}{\alpha + \alpha\xi + \xi}. \quad (30)$$

Accordingly, the subset of state space corresponding to stationary asperities decreases with the degree of coupling between the asperities and with the asymmetry of the system ($\beta \rightarrow 0$). As tectonic loading takes place, the orbit of the system lies within \mathbf{Q} . Eventually, the condition for the failure of asperity 1 (on Line 1), asperity 2 (on Line 2) or both asperities (at point P) is reached, giving rise to a seismic event.

3 The Dynamic Modes

The fault dynamics can be described in terms of four dynamic modes, each associated with a different system of ordinary differential equations: a sticking mode (mode 00), corresponding to stationary asperities, and three slipping modes, corresponding to the failure of asperity 1 (mode 10), the failure of asperity 2 (mode 01) and the simultaneous failure of both asperities (mode 11).

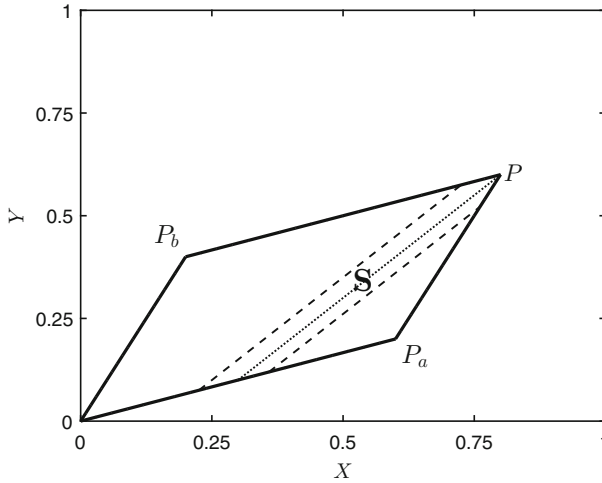


Fig. 2 The sticking region of the system: a parallelogram Q ($\alpha = 1, \beta = 0.5, \gamma = 1, \epsilon = 0.7, \xi = 2$). The subset S from which events involving the simultaneous slip of the asperities take place is indicated. The dashed lines correspond to $p = p_1$ (right) and $p = p_2$ (left), the dotted line to $p = p_0$

For later use, the frequencies

$$\omega_1 = \sqrt{1 + \alpha - \frac{\gamma^2}{4}}, \quad \omega_2 = \sqrt{1 + \alpha' - \frac{\gamma^2}{4}}, \tag{31}$$

$$\omega_a = \sqrt{1 - \frac{\gamma^2}{4}}, \quad \omega_b = \sqrt{1 + \alpha + \alpha' - \frac{\gamma^2}{4}}, \tag{32}$$

are introduced. In the following, the equations of motion (17) and (18) for the four dynamic modes are specialized and their solution in the case of underdamping is provided: this condition corresponds to $\gamma \leq 2$, implying that the velocity dependent terms are small with respect to dynamic frictions. It is assumed that each mode begins at $T = 0$.

3.1 Stationary Asperities (Mode 00)

The equations of motion are

$$\ddot{X} = 0, \quad \ddot{Y} = 0, \tag{33}$$

with initial conditions

$$X(0) = \bar{X}, \quad Y(0) = \bar{Y}, \quad \dot{X}(0) = V, \quad \dot{Y}(0) = V, \tag{34}$$

where \bar{X} and \bar{Y} are the slip deficits of asperities 1 and 2, respectively, at the beginning of the interseismic interval. Because of tectonic loading, their initial rate of change is the velocity of tectonic plates V . The solutions are

$$X(T) = \bar{X} + VT, \quad Y(T) = \bar{Y} + VT, \tag{35}$$

where $T \geq 0$. Equations (35) are the parametric equations of the line

$$Y = X + p, \tag{36}$$

where

$$p = \bar{Y} - \bar{X}. \tag{37}$$

This line is the orbit of the system in the sticking region **Q** in mode 00.

3.2 Failure of Asperity 1 (Mode 10)

The equations of motion are

$$\ddot{X} + \gamma \dot{X} + (1 + \alpha)X - \alpha Y - \epsilon = 0, \tag{38}$$

$$\ddot{Y} = 0. \tag{39}$$

The system may enter mode 10 from mode 11 or from mode 00.

(a) In the case $11 \rightarrow 10$, initial conditions are

$$X(0) = \bar{X}, \quad Y(0) = \bar{Y}, \quad \dot{X}(0) = \bar{V}, \quad \dot{Y}(0) = 0, \tag{40}$$

where \bar{X} and \bar{Y} are the slip deficits of asperities 1 and 2, respectively, when asperity 1 starts slipping alone at a certain rate \bar{V} and asperity 2 stops slipping, so that its velocity is null. The solution is

$$X(T) = \bar{X} - \frac{\bar{U}_1}{2} + \left[\frac{\bar{U}_1}{2} \cos \omega_1 T + \frac{1}{\omega_1} \left(\frac{\gamma}{4} \bar{U}_1 + \bar{V} \right) \sin \omega_1 T \right] e^{-\frac{\gamma}{2} T}, \tag{41}$$

$$Y(T) = \bar{Y}, \tag{42}$$

where

$$\bar{U}_1 = 2 \left(\bar{X} - \frac{\alpha \bar{Y} + \epsilon}{1 + \alpha} \right). \tag{43}$$

If the orbit does not reach Line 2 during the mode, the slip duration can be calculated from the condition $\dot{X}(T) = 0$, yielding

$$T_{1a} = \frac{1}{\omega_1} \left[\pi + \arctan \frac{2\omega_1 \bar{V}}{(1 + \alpha)\bar{U}_1 + \gamma \bar{V}} \right]. \tag{44}$$

The final slip amplitude is then

$$U_{1a} = \bar{X} - X(T_{1a}) = \frac{\bar{U}_1}{2} + \sqrt{\frac{\bar{U}_1^2}{4} + \frac{\bar{V}^2}{1 + \alpha} + \frac{\gamma \bar{U}_1 \bar{V}}{2(1 + \alpha)}} e^{-\frac{\gamma}{2} T_{1a}}. \tag{45}$$

If instead the orbit reaches Line 2 during the mode, the system enters again mode 11.

(b) In the case $00 \rightarrow 10$, initial conditions are

$$X(0) = \bar{X}, \quad Y(0) = \bar{Y}, \quad \dot{X}(0) = 0, \quad \dot{Y}(0) = 0, \tag{46}$$

where \bar{X} and \bar{Y} are related by (23) and the initial velocity of both asperities is null. The solution reduces to

$$X(T) = \bar{X} - \frac{U}{2} \left[1 - \left(\cos \omega_1 T + \frac{\gamma}{2\omega_1} \sin \omega_1 T \right) e^{-\frac{\gamma}{2} T} \right], \tag{47}$$

$$Y(T) = \bar{Y}, \tag{48}$$

where

$$U = 2 \frac{1 - \epsilon}{1 + \alpha}. \tag{49}$$

If the orbit does not reach Line 2 during the mode, the mode duration is

$$T_{1b} = \frac{\pi}{\omega_1}, \tag{50}$$

while the final slip amplitude is

$$U_{1b} = \kappa_1 U, \tag{51}$$

where

$$\kappa_1 = \frac{1}{2} \left(1 + e^{-\frac{\gamma}{2} T_{1b}} \right). \tag{52}$$

Hence, U_{1b} is the maximum slip in mode 10. If the orbit reaches Line 2 before time T_{1b} has elapsed, the system passes to mode 11. In this case, the slip duration and amplitude are smaller than T_{1b} and U_{1b} , respectively.

3.3 Failure of Asperity 2 (Mode 01)

The equations of motion are

$$\ddot{X} = 0, \tag{53}$$

$$\ddot{Y} + \gamma \dot{Y} + (1 + \alpha')Y - \alpha'X - \beta\epsilon = 0. \tag{54}$$

The system may enter mode 01 from mode 11 or from mode 00.

(a) In the case $11 \rightarrow 01$, initial conditions are

$$X(0) = \bar{X}, \quad Y(0) = \bar{Y}, \quad \dot{X}(0) = 0, \quad \dot{Y}(0) = \bar{V}, \tag{55}$$

where \bar{X} and \bar{Y} are the slip deficits of asperities 1 and 2, respectively, when asperity 2 starts slipping alone at a certain rate \bar{V} and asperity 1 stops slipping, so that its velocity is null. The solution is

$$X(T) = \bar{X}, \quad (56)$$

$$Y(T) = \bar{Y} - \frac{\bar{U}_2}{2} + \left[\frac{\bar{U}_2}{2} \cos \omega_2 T + \frac{1}{\omega_2} \left(\frac{\gamma}{4} \bar{U}_2 + \bar{V} \right) \sin \omega_2 T \right] e^{-\frac{\gamma}{2} T}, \quad (57)$$

where

$$\bar{U}_2 = 2 \left(\bar{Y} - \frac{\alpha' \bar{X} + \beta \epsilon}{1 + \alpha'} \right). \quad (58)$$

If the orbit does not reach Line 1 during the mode, the slip duration can be calculated from the condition $\dot{Y}(T) = 0$, yielding

$$T_{2a} = \frac{1}{\omega_2} \left[\pi + \arctan \frac{2\omega_2 \bar{V}}{(1 + \alpha') \bar{U}_2 + \gamma \bar{V}} \right]. \quad (59)$$

The final slip amplitude is then

$$U_{2a} = \bar{Y} - Y(T_{2a}) = \frac{\bar{U}_2}{2} + \sqrt{\frac{\bar{U}_2^2}{4} + \frac{\bar{V}^2}{1 + \alpha'} + \frac{\gamma \bar{U}_2 \bar{V}}{2(1 + \alpha')}} e^{-\frac{\gamma}{2} T_{2a}}. \quad (60)$$

If instead the orbit reaches Line 1 during the mode, the system enters again mode 11.

(b) In the case $00 \rightarrow 01$, initial conditions are

$$X(0) = \bar{X}, \quad Y(0) = \bar{Y}, \quad \dot{X}(0) = 0, \quad \dot{Y}(0) = 0, \quad (61)$$

where \bar{X} and \bar{Y} are related by (24) and the initial velocity of both asperities is null. The solution reduces to

$$X(T) = \bar{X}, \quad (62)$$

$$Y(T) = \bar{Y} - \frac{\beta U'}{2} \left[1 - \left(\cos \omega_2 T + \frac{\gamma}{2\omega_2} \sin \omega_2 T \right) e^{-\frac{\gamma}{2} T} \right], \quad (63)$$

where

$$U' = 2 \frac{1 - \epsilon}{1 + \alpha'}. \quad (64)$$

If the orbit does not reach Line 1 during the mode, the mode duration is

$$T_{2b} = \frac{\pi}{\omega_2}, \quad (65)$$

while the final slip amplitude is

$$U_{2b} = \beta \kappa_2 U', \quad (66)$$

where

$$\kappa_2 = \frac{1}{2} \left(1 + e^{-\frac{\gamma}{2} T_{2b}} \right). \quad (67)$$

Hence, U_{2b} is the maximum slip in mode 01. If the orbit reaches Line 1 before time T_{2b} has elapsed, the system passes to mode 11. In this case, the slip duration and amplitude are smaller than T_{2b} and U_{2b} , respectively.

3.4 Simultaneous Asperity Failure (Mode 11)

The equations of motion are

$$\ddot{X} + \gamma \dot{X} + (1 + \alpha)X - \alpha Y - \epsilon = 0, \tag{68}$$

$$\ddot{Y} + \gamma \dot{Y} + (1 + \alpha')Y - \alpha' X - \beta \epsilon = 0. \tag{69}$$

The system may enter mode 11 from mode 10, 01 or 00. In all cases, the solution is

$$X(T) = \epsilon X_P + (A \sin \omega_a T + B \cos \omega_a T + C \sin \omega_b T + D \cos \omega_b T) e^{-\frac{\gamma}{2} T}, \tag{70}$$

$$Y(T) = \epsilon Y_P + \left(A \sin \omega_a T + B \cos \omega_a T - \frac{1}{\xi} C \sin \omega_b T - \frac{1}{\xi} D \cos \omega_b T \right) e^{-\frac{\gamma}{2} T}, \tag{71}$$

where the constants A, B, C, D depend on the initial conditions (“Appendix A”). Mode 11 terminates at time $T = T_{11}$ when one of the asperities stops. Hence the mode duration is

$$T_{11} = \min(T_X, T_Y), \tag{72}$$

where T_X and T_Y are respectively the smallest positive solutions of the equations

$$\dot{X}(T) = 0, \quad \dot{Y}(T) = 0. \tag{73}$$

4 Subsets of the Sticking Region

During the interseismic intervals, the state of the fault is represented by a point (X, Y) in the sticking region \mathbf{Q} . The orbit of the system is given by line (36) starting at a point $P_0 = (\bar{X}, \bar{Y})$. The kind of seismic event generated by the fault depends on the subset of \mathbf{Q} which the representative point P_0 belongs to. In fact, it depends exclusively on the value of the variable p defined in (37); therefore, the subsets of \mathbf{Q} are defined by the values of p .

(1) A major subdivision of \mathbf{Q} is the orbit through P , driving the fault from mode 00 to mode 11. This orbit belongs to the line

$$Y = X + p_0, \tag{74}$$

where

$$p_0 = Y_P - X_P. \tag{75}$$

Thanks to (29), it results

$$p_0 = \frac{(\beta - 1)\xi}{\alpha + \alpha\xi + \xi}. \tag{76}$$

Line (74) divides \mathbf{Q} in two subsets producing events with initial mode 10 ($p < p_0$) and 01 ($p > p_0$), respectively. In the particular case $p = p_0$, the fault will produce a two-mode event 11-01: this is the largest seismic event predicted by the model.

(2) Next, the subset \mathbf{S} of \mathbf{Q} from which the fault produces slipping of one asperity followed by the simultaneous motion of both of them is determined. This subset is defined by the values of p belonging to the interval $[p_1, p_2]$. It is shown in Fig. 2. Initial states that are outside the subset \mathbf{S} produce events that are made of a single mode 10 or 01, corresponding to $p < p_1$ and $p > p_2$, respectively. In this case, no simultaneous asperity slip is possible. For later use, let \mathbf{S}_1 and \mathbf{S}_2 be the subsets of \mathbf{S} below and above line (74), respectively.

In view of the following discussion, we recall that the maximum slip of asperity 1 during mode 10 is $\kappa_1 U$, corresponding to the slip duration T_{1b} , whereas the maximum slip of asperity 2 during mode 01 is $\beta\kappa_2 U'$, corresponding to the slip duration T_{2b} .

(a) The value of p_1 is calculated considering an event starting with mode 10. The lower margin of \mathbf{S} is the line $Y = X + p_1$ causing asperity 1 to trigger the motion of asperity 2 after completing mode 10. The coordinates of point P_1 , where mode 10 starts, are

$$X_1 = 1 + \alpha p, \quad Y_1 = 1 + (1 + \alpha)p. \quad (77)$$

The coordinates of point P_2 , where mode 10 ends, are

$$X_2 = X_1 - \kappa_1 U, \quad Y_2 = Y_1. \quad (78)$$

Since it must belong to Line 2, it results

$$p_1 = \frac{(\beta - 1)\xi - \alpha\kappa_1 U}{\alpha + \xi + \alpha\xi}. \quad (79)$$

The circumstances under which mode 01 starting at P_2 is followed by other slipping modes are investigated. If the orbit of mode 01 does not meet Line 1 before time T_{2b} has elapsed, the slip of asperity 2 terminates at point P_3 with coordinates

$$X_3 = X_2, \quad Y_3 = Y_2 - \beta\kappa_2 U'. \quad (80)$$

If P_3 belongs to Line 1, mode 01 is followed by a second phase of mode 10. This situation corresponds to a specific value of β , namely

$$\beta = \beta_1 = \frac{(\alpha + \xi)\kappa_1}{\alpha\xi\kappa_2}. \quad (81)$$

In the particular case in which $\beta > \beta_1$, the orbit of mode 01 reaches Line 1 before time T_{2b} has elapsed and the system enters mode 11. The different cases are summarized in Table 1.

(b) The value of p_2 is calculated considering an event starting with mode 01. The upper margin of \mathbf{S} is the line $Y = X + p_2$ causing asperity 2 to trigger the motion of asperity 1 after completing mode 01. The coordinates of point P_1 , where mode 01 starts, are

Table 1 Seismic events resulting from $p = p_1$ defined in (79), as a function of β . The particular value $\beta = \beta_1$ is defined in (81)

	$\beta < \beta_1$	$\beta = \beta_1$	$\beta > \beta_1$
Seismic event	10-01	10-01-10	10-01-11-

Table 2 Seismic events resulting from $p = p_2$ defined in (84), as a function of β . The particular value $\beta = \beta_2$ is defined in (86)

	$\beta < \beta_2$	$\beta = \beta_2$	$\beta > \beta_2$
Seismic event	01-10-11-	01-10-01	01-10

$$X_1 = \beta - (1 + \alpha')p, \quad Y_1 = \beta - \alpha'p. \tag{82}$$

The coordinates of point P_2 , where mode 01 ends, are

$$X_2 = X_1, \quad Y_2 = Y_1 - \beta\kappa_2U'. \tag{83}$$

Since it must belong to Line 1, it results

$$p_2 = \frac{(\beta - 1)\xi + \alpha\beta\xi\kappa_2U'}{\alpha + \xi + \alpha\xi}. \tag{84}$$

The circumstances under which mode 10 starting at P_2 is followed by other slipping modes are investigated. If the orbit of mode 10 does not meet Line 2 before time T_{1b} has elapsed, the slip of asperity 1 terminates at point P_3 with coordinates

$$X_3 = X_2 - \kappa_1U, \quad Y_3 = Y_2. \tag{85}$$

If P_3 belongs to Line 2, mode 10 is followed by a second phase of mode 01. This situation corresponds to a specific value of β , namely

$$\beta = \beta_2 = \frac{\alpha\kappa_1}{\xi(1 + \alpha)\kappa_2}. \tag{86}$$

In the particular case in which $\beta < \beta_2$, the orbit of mode 10 reaches Line 2 before time T_{1b} has elapsed and the system enters mode 11. The different cases are summarized in Table 2.

For the sake of simplicity, the condition

$$\beta_2 < \beta < \beta_1, \tag{87}$$

will be assumed throughout the rest of the paper. Accordingly, the stress distribution associated with $p = p_1$ and $p = p_2$ correspond to two-mode events 10-01 and 01-10, respectively.

5 Moment Rates and Moment Rate Spectra

A seismic event generated by the fault may involve one or more slipping modes. If n is the number of slipping modes in the event, let $P_i = (X_i, Y_i)$ be the representative point of the system at the onset of the i -th mode ($i = 1, 2, \dots, n$).

Each event is described by a seismic moment $m(t)$ or, in nondimensional form

$$M(T) = \frac{K_1}{f_{s1}^2} m(t). \quad (88)$$

As a reference, the seismic moment M_1 that is released in a one-mode event 10 when $\gamma = 0$ is considered. The moment rate of an n -mode event is then

$$\dot{M}(T) = M_1 \frac{\Delta \dot{X} + \Delta \dot{Y}}{U}, \quad (89)$$

where $\Delta \dot{X}$ and $\Delta \dot{Y}$ are the slip rates of the asperities during the event (Dragonì and Tallarico 2016). The final seismic moment is

$$M_0 = M_1 \frac{U_1 + U_2}{U}, \quad (90)$$

where

$$U_1 = X_1 - X_{n+1}, \quad U_2 = Y_1 - Y_{n+1}, \quad (91)$$

are the final slip amplitudes of the asperities.

The moment rates of events involving the failure of a single asperity or the consecutive, but separate, failures of the two asperities, are considered. These are the more frequent events and completely analytical expressions can be obtained for them.

(1) One-mode events. If an earthquake is produced by the failure of asperity 1, (89) yields

$$\dot{M}(T) = M_1 \frac{1 + \alpha}{2\omega_1} \sin \omega_1 T e^{-\frac{\gamma}{2} T}, \quad (92)$$

with $0 \leq T \leq T_{1b}$. The final seismic moment is

$$M_0 = \kappa_1 M_1. \quad (93)$$

If the earthquake is produced by the failure of asperity 2, (89) yields

$$\dot{M}(T) = M_1 \frac{1 + \alpha}{2\omega_2} \beta \sin \omega_2 T e^{-\frac{\gamma}{2} T}, \quad (94)$$

with $0 \leq T \leq T_{2b}$. The final seismic moment is

$$M_0 = \frac{1 + \alpha}{1 + \alpha'} \beta \kappa_2 M_1. \quad (95)$$

(2) Two-mode events 10-01/01-10. If the sequence of slipping modes is 10-01, the moment rate is

$$\dot{M}(T) = M_1 \frac{1 + \alpha}{2} \begin{cases} \frac{1}{\omega_1} \sin \omega_1 T e^{-\frac{\gamma}{2} T}, & 0 \leq T \leq T_{1b} \\ \frac{\beta}{\omega_2} \sin \omega_2 (T - T_{1b}) e^{-\frac{\gamma}{2} (T - T_{1b})}, & T_{1b} \leq T \leq \Delta T \end{cases} \tag{96}$$

where

$$\Delta T = T_{1b} + T_{2b}. \tag{97}$$

If the sequence of slipping modes is 01-10, the expression is straightforward. In both cases, the final seismic moment is

$$M_0 = \left(\kappa_1 + \frac{1 + \alpha}{1 + \alpha'} \beta \kappa_2 \right) M_1. \tag{98}$$

Following Dragoni and Santini (2015), the nondimensional moment rate spectrum of a seismic event can be calculated as

$$S(\Omega) = \left| \int_0^{\Delta T} \dot{M}(T) e^{-i\Omega T} dT \right|, \tag{99}$$

where ΔT is the duration of the event and Ω is a nondimensional frequency, defined from the angular frequency ω of the emitted waves as

$$\Omega = \sqrt{\frac{\mu_1}{K_1}} \omega. \tag{100}$$

The spectrum can be calculated analytically for one-mode events 10 or 01 and for two-mode events 10-01 or 01-10: for the sake of simplicity, only the spectrum of one-mode events is shown.

(1) For a one-mode event 10, $\Delta T = T_{1b}$ and it results

$$S(\Omega) = M_1 \frac{1 + \alpha}{2} \sqrt{\frac{1 + 2e^{-\frac{\gamma}{2} T_{1b}} \cos \Omega T_{1b} + e^{-\gamma T_{1b}}}{(1 + \alpha - \Omega^2)^2 + \gamma^2 \Omega^2}}, \tag{101}$$

a result that was already given by Dragoni and Santini (2015). Its value for $\Omega = 0$ is

$$S_0 = M_0, \tag{102}$$

where M_0 is given by (93), and its envelope for $\Omega \rightarrow \infty$ is

$$S_\infty(\Omega) = \frac{1 + \alpha}{\Omega^2} M_0. \tag{103}$$

The nondimensional corner frequency is

$$\Omega_c = \sqrt{1 + \alpha}, \tag{104}$$

and its dimensional value is

$$\omega_c = \frac{T_{1b}}{t'} \Omega_c, \tag{105}$$

where t' is the observed event duration.

(2) For a one-mode event 01, $\Delta T = T_{2b}$ and the spectrum is

$$S(\Omega) = M_1 \frac{1 + \alpha}{2} \beta \sqrt{\frac{1 + 2e^{-\frac{\gamma}{2} T_{2b}} \cos \Omega T_{2b} + e^{-\gamma T_{2b}}}{(1 + \alpha' - \Omega^2)^2 + \gamma^2 \Omega^2}}. \tag{106}$$

Its value for $\Omega = 0$ is

$$S_0 = \frac{1 + \alpha}{1 + \alpha'} \beta \kappa_2 M_1 = M_0, \tag{107}$$

where M_0 is given by (95), and its envelope for $\Omega \rightarrow \infty$ is

$$S_\infty(\Omega) = \frac{1 + \alpha'}{\Omega^2} M_0. \tag{108}$$

The nondimensional corner frequency is

$$\Omega_c = \sqrt{1 + \alpha'}, \tag{109}$$

and its dimensional value is

$$\omega_c = \frac{T_{2b}}{t'} \Omega_c. \tag{110}$$

6 Discussion

In this section, the influence of the difference between the asperity areas on several features of the model is investigated. For the sake of the present discussion, it is assumed that the size of asperity 1 remains fixed, whereas asperity 2 can be smaller ($\xi < 1$) or larger ($\xi > 1$). In the following, very small or large values of the parameter ξ (e.g. $\xi = 0.1$ or $\xi = 10$) are not considered, since they are not significant: in fact, they would imply that one asperity is considerably smaller than the other, so that its contribution to fault dynamics and moment release during a seismic event would be negligible. First, the evolution of the tangential forces on the asperities during a global stick phase is considered. Combining (20) with (35), the forces F_1 and F_2 during mode 00 are

$$F_1(T) = -\bar{X} + \alpha p - VT, \quad F_2(T) = -\xi \bar{Y} - \alpha p - \xi VT. \tag{111}$$

Accordingly, the forces on the asperities do not evolve with the same rate, since

$$\dot{F}_1 = -V, \quad \dot{F}_2 = -\xi V. \tag{112}$$

In conclusion, $|\dot{F}_2| > |\dot{F}_1|$ if asperity 2 is larger than asperity 1, and vice-versa.

A significant implication of (111) concerns the meaning of the variable p defined in (37). In fact, the difference

$$F_1(T) - F_2(T) = -\bar{X} + \xi\bar{Y} + 2\alpha p + (\xi - 1)VT, \tag{113}$$

does not remain constant during an interseismic interval, except for the limit case $\xi = 1$, for which it results

$$F_1 - F_2 = (1 + 2\alpha)p. \tag{114}$$

As a result, the variable p no longer describes the stress inhomogeneity on the fault in a univocal way (Dragoni and Santini 2012). Nevertheless, it still controls which asperity fails the first in a seismic event, as shown when describing the subsets of the sticking region. Next, the dependence of slip duration and amplitude on the size of the asperities is investigated. The parameter ξ appears in the solutions of dynamic modes involving the slip of asperity 2, as shown when discussing mode 01 and mode 11. For the sake of simplicity, only one-mode events 01 are considered. Figure 3 shows the slip duration (65) and final slip amplitude (66) in a one-mode event 01, as functions of ξ . They are expressed in units of the slip duration (50) and final slip amplitude (51) associated with a one-mode event 10, respectively. Notice that the slip durations T_{1b} and T_{2b} coincide in the limit case $\xi = 1$ (asperities of equal areas), whereas $U_{2b} < U_{1b}$ for any value of ξ , since asperity 2 is assumed to be weaker than asperity 1. In turn, the source function of the event is affected by ξ : for larger values of this parameter, the source function reaches a larger maximum value that is delayed in time, as shown in Fig. 4.

Next, the effect of the parameter ξ on the sticking region \mathbf{Q} of the system is investigated. The area $A_{\mathbf{Q}}$ of the sticking region was given in (30): it is shown in Fig. 5 as a function of ξ , in units of the area $A_{\mathbf{Q}}^*$ corresponding to the limit case $\xi = 1$ (asperities of equal areas). The graph clearly shows that the area $A_{\mathbf{Q}}$ is smaller than the area $A_{\mathbf{Q}}^*$ for $\xi < 1$; the opposite holds for $\xi > 1$. As a matter of fact, the overall inertia of the system decreases when $\xi < 1$ and the set of states corresponding to stationary asperities is reduced in turn; the opposite holds when $\xi > 1$. Figure 6a shows the area $A_{\mathbf{S}}$ of the subset \mathbf{S} of the sticking region from which events involving the simultaneous slip of the asperities take place, as a function of ξ . A deeper insight is presented in Fig. 6b, showing the dependence on ξ of the areas $A_{\mathbf{S}_1}$ and $A_{\mathbf{S}_2}$ of the subsets \mathbf{S}_1 and \mathbf{S}_2 . On the whole, as the overall area of the asperities gets larger, the probability that the system gives rise to events involving the simultaneous slip of the asperities decreases. More specifically, the subset \mathbf{S}_1 decreases with ξ , since the slip of asperity 1 is less likely to trigger the failure of asperity 2 if its size grows. On the contrary, the subset \mathbf{S}_2 increases with ξ , since a larger size entails a larger slip amplitude of asperity 2 and, in turn, a larger stress transfer to asperity 1; as a result, it is easier for the slip of asperity 2 to trigger the failure of asperity 1. Notice that there exists a particular value of ξ in correspondence to which \mathbf{S}_1 and \mathbf{S}_2 are equal to each other. This value must be evaluated numerically and depends on the particular combination of the parameters α , β , γ and ϵ .

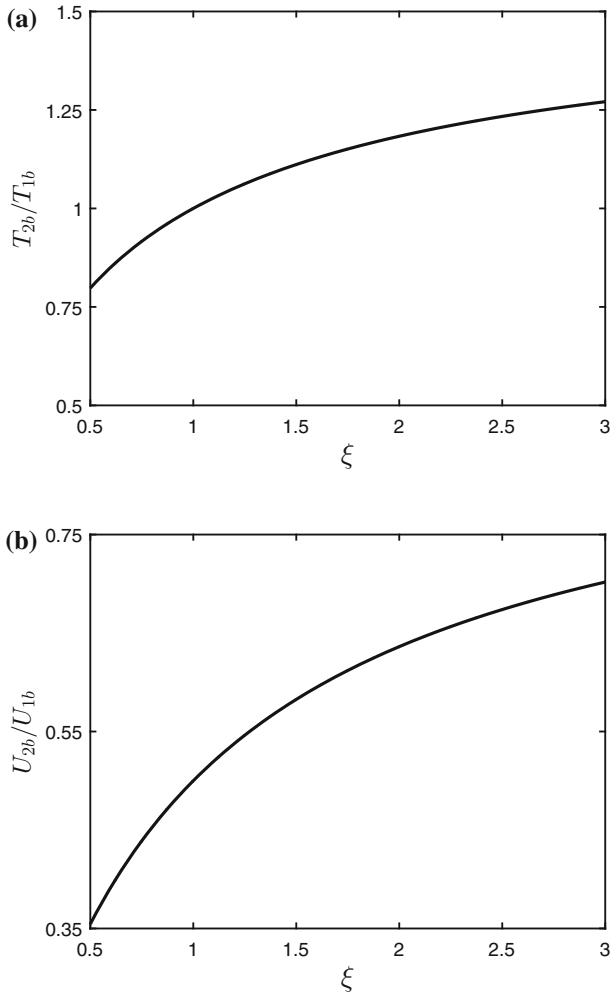


Fig. 3 **a** Slip duration and **b** final slip amplitude in a one-mode event 01, as functions of ξ ($\alpha = 1$, $\beta = 0.5$, $\gamma = 1$, $\epsilon = 0.7$). They are normalized to the slip duration and final slip amplitude associated with a one-mode event 10, respectively

In order to show the influence of the asperity area on the radiation of elastic waves during fault slip, the moment rate spectrum (106) associated with one-mode events 01 is considered first. It is shown in Fig. 7 for different values of the parameter ξ . As asperity 2 gets larger, the corner frequency (109) diminishes, so that the content of relatively high frequencies is reduced. Next, the seismic efficiency of the fault is discussed. It is defined as the ratio

$$\eta = \frac{\Delta R}{\Delta W} \quad (115)$$

between the nondimensional seismic energy ΔR and the nondimensional total energy change ΔW associated with a seismic event. An event made up of n slipping modes

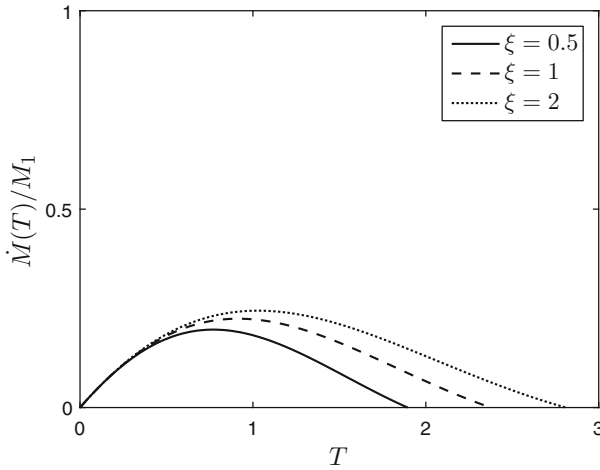


Fig. 4 Source function of a one-mode event 01 for different values of the parameter ξ ($\alpha = 1, \beta = 0.5, \gamma = 1, \epsilon = 0.7$)

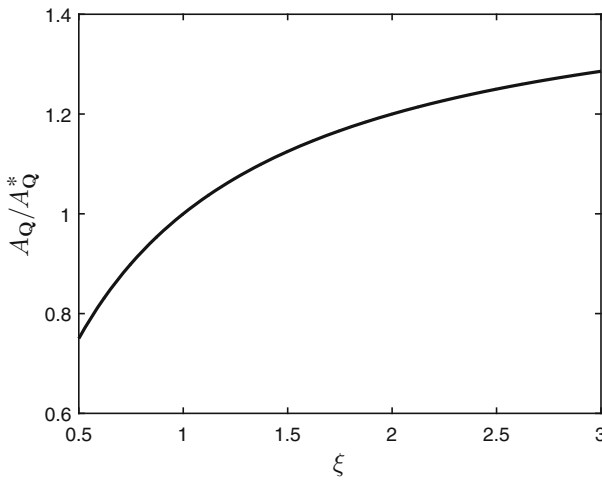


Fig. 5 The area A_Q of the sticking region Q , as a function of the parameter ξ ($\alpha = 1, \beta = 0.5$). It is normalized to the area A_Q^* corresponding to $\xi = 1$

starting at time T_i ($i = 1, 2, \dots, n$), when the state of the system is (X_i, Y_i) , is considered. Following Dragoni and Santini (2015), the seismic energy released during the event can be calculated as

$$\Delta R = -\gamma \sum_{i=1}^n \int_{T_i}^{T_{i+1}} (\dot{X}_i^2 + \xi \dot{Y}_i^2) dT, \tag{116}$$

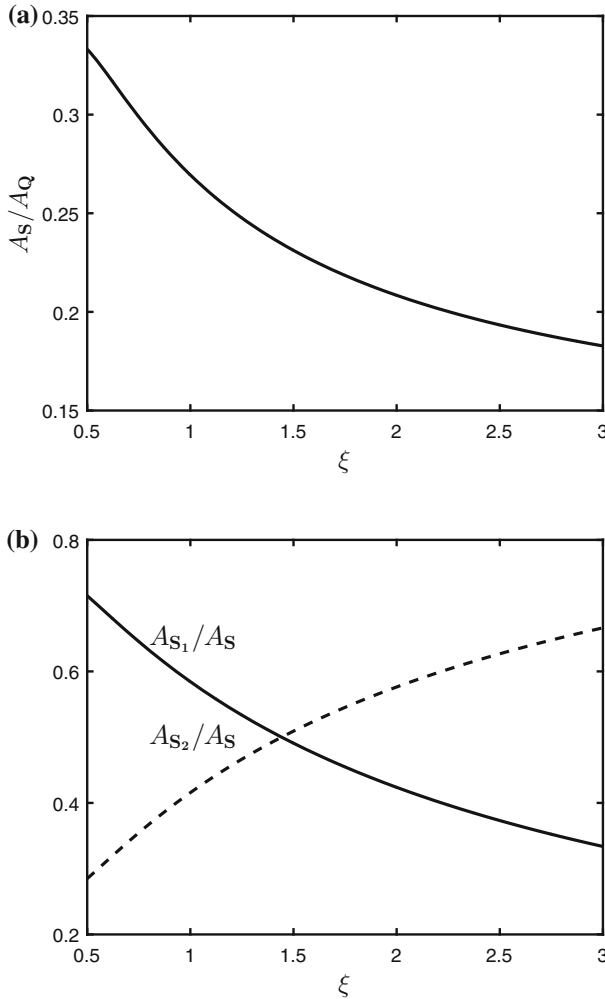


Fig. 6 **a** The area A_S of the subset S of the sticking region Q and **b** the areas A_{S_1} and A_{S_2} of its subsets S_1 and S_2 , as functions of the parameter ξ ($\alpha = 1, \beta = 0.5, \gamma = 1, \epsilon = 0.7$)

where \dot{X}_i and \dot{Y}_i are the slip rates of the asperities during the event. During a sticking mode, the total energy of the system is

$$W(X, Y) = \frac{1}{2}(X^2 + \xi Y^2) + \frac{1}{2}\alpha(X - Y)^2. \tag{117}$$

Accordingly, the total energy change in the event is given by

$$\Delta W = W(X_1 - U_1, Y_1 - U_2) - W(X_1, Y_1), \tag{118}$$

where U_1 and U_2 are the final slip amplitudes (91) of the asperities.

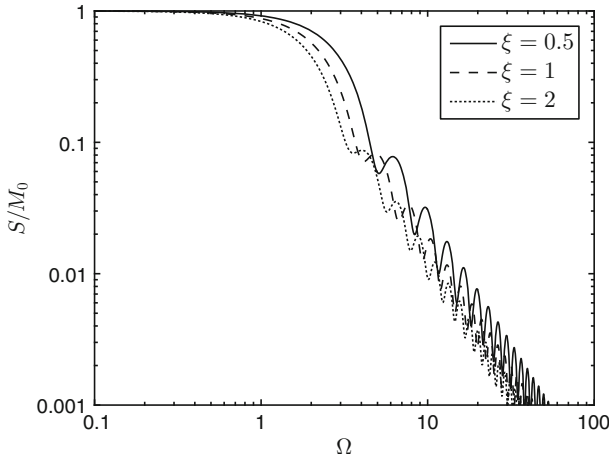


Fig. 7 Moment rate spectrum of a one-mode event 01 for different values of the parameter ξ ($\alpha = 1, \beta = 0.5, \gamma = 1$)

In the case of a two-mode event 10-01, it results

$$T_1 = 0, \quad T_2 = T_{1b}, \quad T_3 = T_{1b} + T_{2b}, \tag{119}$$

$$U_1 = U_{1b}, \quad U_2 = U_{2b}, \tag{120}$$

and the initial state is given by (77) with $p = p_1$ defined in (79). In the case of a two-mode event 01-10, it results

$$T_1 = 0, \quad T_2 = T_{2b}, \quad T_3 = T_{1b} + T_{2b}, \tag{121}$$

$$U_1 = U_{1b}, \quad U_2 = U_{2b} \tag{122}$$

and the initial state is given by (82) with $p = p_2$ defined in (84). The seismic efficiency calculated from (115) is the same for the two events. Its analytical expression is too complicated to be reported here: its dependence on ξ is shown in Fig. 8. It can be concluded that the seismic efficiency associated with events due to the consecutive, but separate failures of the asperities increases with the overall size of the asperities.

7 An Application: The 2007 Pisco, Peru, Earthquake

The M_w 8.0 Pisco (Peru) earthquake of 15 August 2007 occurred as the result of thrust faulting at the interface between the Nazca and South American plates, with a seismic moment estimated between 1.8 and 2×10^{21} Nm (Lay et al. 2010). The slip distribution inferred from the joint inversion of teleseismic body waves and InSAR data indicates the presence of two distinct asperities (Sladen et al. 2010): a shallower, larger one (asperity 1), where the maximum coseismic slip was attained, and a deeper, smaller one (asperity 2). The earthquake initiated with the slip of asperity 2, followed by the slip of asperity 1 after a brief time interval.

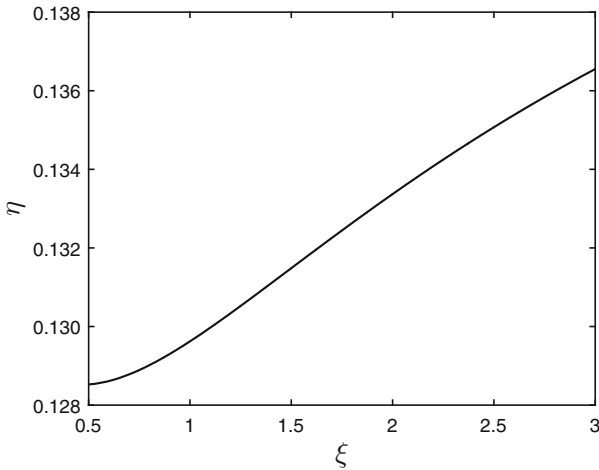


Fig. 8 Seismic efficiency associated with two-mode events 10-01 and 01-10, as a function of the parameter ξ ($\alpha = 1$, $\beta = 0.5$, $\gamma = 1$, $\epsilon = 0.7$)

The two phases of the earthquake were treated as distinct events by Lay et al. (2010), who estimated seismic moments $m_1 = 1.2 \times 10^{21}$ Nm and $m_2 = 3.5 \times 10^{20}$ Nm for the slip of asperity 1 and 2, respectively. With an average rigidity $\mu = 30$ GPa and assuming $A_1 = 4200$ km² and $A_2 = 2400$ km² for the area of asperity 1 and 2, respectively, the average slips of asperities 1 and 2 are, respectively

$$u_1 = \frac{m_1}{\mu A_1} = 9.5 \text{ m}, \quad u_2 = \frac{m_2}{\mu A_2} = 4.8 \text{ m}, \quad (123)$$

where the definition of scalar seismic moment was exploited. Finally, it is assumed that the relative velocity of tectonic plates at the Peru trench is $v = 6$ cm a⁻¹ (Sladen et al. 2010) and that the fault is subject to a shear strain rate $\dot{\epsilon} = 10^{-15}$ s⁻¹, an average of the values provided for the Peruvian interface between the Nazca and South American plates by the GEM Strain Rate Model. With the data listed above, the parameters of the model are evaluated. From (14), $\alpha = 0.2$. The value of β can be estimated from the ratio u_2/u_1 between the slips of the asperities (Dragoni and Santini 2012): accordingly, $\beta = 0.5$. The best fit with the observed source function of the earthquake is obtained with $\gamma = 1.3$, a value corresponding to a seismic efficiency $\eta \simeq 0.16$. It is assumed that $\epsilon = 0.7$ (Jaeger and Cook 1976). Finally, the ratio A_2/A_1 yields $\xi = 0.6$.

In terms of the present model, the 2007 earthquake can be described as a two-mode event 01-10 with a finite time interval between the slips of the asperities. Specifically, it is assumed that the slip of asperity 2 takes place over the time interval $t_1 \leq t \leq t_2$, with $t_1 = 0$ s and $t_2 = 38$ s, whereas the slip of asperity 1 takes place over the time interval $t_3 \leq t \leq t_4$, with $t_3 = 60$ s and $t_4 = 105$ s. The action of tectonic loading during the time gap of 22 s that separates the slips of the asperities is excluded, since its effect is negligible over such a short time. Accordingly, the state of the fault at the onset of the earthquake ($t = t_1$) is given by (82), that is

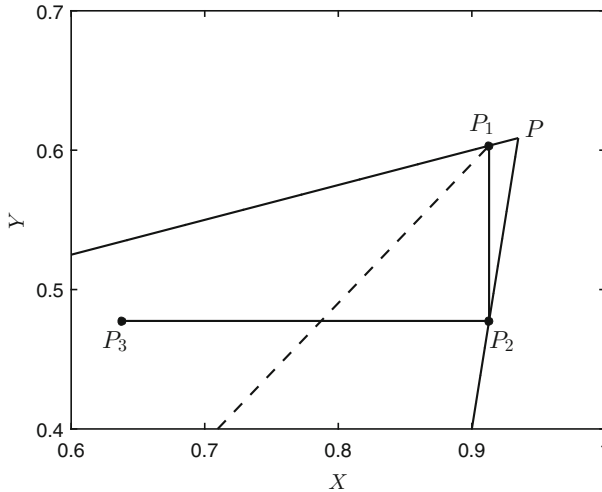


Fig. 9 Orbit of the Pisco (Peru) fault during the 2007 earthquake. The dashed line corresponds to $p = p_2$. The event starts at point P_1 with the slip of asperity 2; the orbit then reaches Line 1 at point P_2 , triggering the slip of asperity 1 up to point P_3 , where the event terminates. For reference, the point P defined in (29) is also shown

$$X_1 = \beta - (1 + \alpha')p_2, \quad Y_1 = \beta - \alpha'p_2, \tag{124}$$

where $p_2 \simeq -0.31$ from (84). At the end of mode 01 ($t = t_2$), the state is given by (83), that is

$$X_2 = X_1, \quad Y_2 = Y_1 - \beta\kappa_2U'. \tag{125}$$

In accordance with the previous assumptions, this is also the state of the fault at the onset of mode 10 ($t = t_3$). Finally, the state at the end of the event ($t = t_4$) is given by (85), that is

$$X_3 = X_2 - \kappa_1U, \quad Y_3 = Y_2. \tag{126}$$

The orbit of the system during the earthquake is shown in Fig. 9.

Next, the observed seismic moment rate is reproduced. In dimensional form, the moment rate predicted by the model is

$$\dot{m}(t) = m_1^0 \frac{1 + \alpha}{2} \begin{cases} \frac{\beta\chi_2}{\omega_2} \sin \omega_2\chi_2(t - t_1) e^{-\frac{\gamma}{2}\chi_2(t-t_1)}, & t_1 \leq t \leq t_2 \\ \frac{\chi_1}{\omega_1} \sin \omega_1\chi_1(t - t_3) e^{-\frac{\gamma}{2}\chi_1(t-t_3)}, & t_3 \leq t \leq t_4, \end{cases} \tag{127}$$

where

$$\chi_1 = \frac{T_{1b}}{t_4 - t_3}, \quad \chi_2 = \frac{T_{2b}}{t_2 - t_1}, \tag{128}$$

while

$$m_1^0 = \mu A_1 u, \tag{129}$$

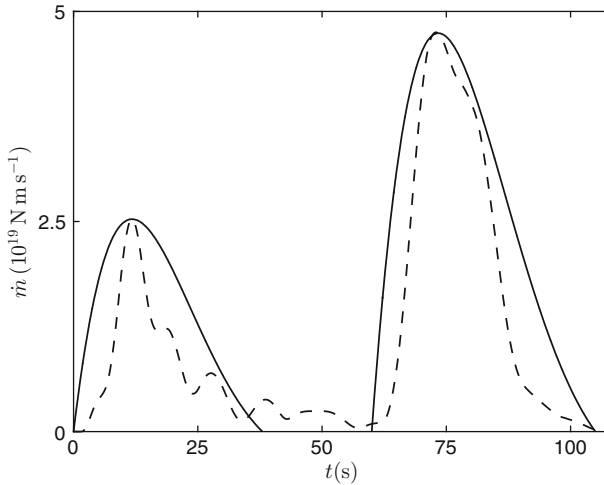


Fig. 10 Modelled source function (solid line) of the 2007 Pisco (Peru) earthquake, compared with the observed source function (dashed line) reported by Sladen et al. (2010)

is the seismic moment released by asperity 1 in the limit case $\gamma = 0$: accordingly, it results $u = u_1/\kappa_1$. The modelled moment rate is shown in Fig. 10 together with the observed moment rate reported by Sladen et al. (2010). The two main peaks of the source function and its shape are reasonably well fit by the model. The final seismic moment provided by the model is

$$m_0 = \left(\kappa_1 + \frac{1 + \alpha}{1 + \alpha'} \beta \kappa_2 \right) m_1^0 \simeq 1.7 \times 10^{21} \text{ Nm}, \quad (130)$$

in good agreement with the observations.

8 Conclusions

A discrete model of a fault containing two asperities characterized by different areas and frictional strengths was presented. The fault is assumed to lie in an elastic shear zone enclosed by two tectonic plates. Owing to tectonic loading, the fault is subject to a constant strain rate.

The leading role of asperities in fault dynamics was exploited to study the fault as a dynamical system with two state variables, corresponding with the slip deficits of the asperities. Four dynamic modes characterize the dynamics of the system: one sticking mode, during which stress is accumulated on the fault and asperities are stationary, and three slipping modes, associated with a seismic event due to the failure of one or both the asperities at a time. Complete analytical solutions for the corresponding equations of motion were provided; subsequently, the expressions of the moment rate functions and seismic spectra associated with the most frequent seismic events were derived.

The type of seismic event generated by the fault can be discriminated from the knowledge of the state of the system at the beginning of the interseismic interval preceding the event. Specifically, the different seismic events predicted by the model correspond with specific values of a variable related with the difference between the slip deficits of the asperities at the beginning of the interseismic interval.

The influence of the different sizes of the asperities on several features of the model was discussed. It was shown that the force rates on the asperities are not equal to each other and that their difference does not remain constant during an interseismic interval, in contrast with the case of asperities of equal areas. Focusing on events associated with the failure of a single asperity, it was shown how the slip duration and amplitude increase with the size of the asperity, while the corner frequency of the seismic spectrum decreases. It was shown that the set of the state space corresponding to stationary asperities grows with the overall area of the asperities; on the contrary, the probability that the system gives rise to events involving the simultaneous slip of the asperities decreases. Focusing on the radiation of elastic waves during events associated with the consecutive, but separate slip of the asperities, it was shown how the related seismic efficiency is affected by the overall size of the asperities.

As an application of the model, the 2007 Pisco, Peru, earthquake was considered. This event was ascribed to the consecutive, but separate, slips of two asperities with significantly different sizes. The earthquake was modelled as a two-mode event starting with the slip of the weaker asperity, followed by the slip of the stronger one after a finite time interval. The state of the fault at the onset of the event was characterized and the orbit of the system during the event was drawn. The modelled moment rate function of the earthquake was found to fit the observations reasonably well.

Online Resources

GEM Strain Rate Model available at <http://gsrm2.unavco.org/gsrn2.html>

Acknowledgements The authors are thankful to the editor Roussos Dimitrakopoulos and to two anonymous referees for their useful comments on the first version of the paper.

A Constants in the Solution for Mode 11

A.1 Case 10 → 11

The initial conditions are

$$X(0) = \bar{X}, \quad Y(0) = \bar{Y}, \quad \dot{X}(0) = \bar{V}, \quad \dot{Y}(0) = 0, \quad (\text{A.1})$$

where \bar{X} and \bar{Y} are the slip deficits of asperities 1 and 2, respectively, when the asperities start slipping together. Asperity 1, which was already slipping at the onset of mode 11, is associated with a certain rate \bar{V} , whereas asperity 2 is initially stationary. The slip deficits \bar{X} and \bar{Y} satisfy the Eq. (24) of Line 2. The constants are

$$A = \frac{1}{\omega_a} \left(\frac{\gamma}{2} B + \frac{1}{1 + \xi} \bar{V} \right), \quad (\text{A.2})$$

$$B = \frac{1}{1 + \xi} [\bar{X} + \xi \bar{Y} - \epsilon (1 + \beta \xi)], \quad (\text{A.3})$$

$$C = \frac{1}{\omega_b} \left(\frac{\gamma}{2} D - \frac{\xi}{1 + \xi} \bar{V} \right), \quad (\text{A.4})$$

$$D = \frac{\xi}{1 + \xi} [\bar{X} - \bar{Y} - \epsilon (X_P - Y_P)]. \quad (\text{A.5})$$

A.2 Case 01 → 11

The initial conditions are

$$X(0) = \bar{X}, \quad Y(0) = \bar{Y}, \quad \dot{X}(0) = 0, \quad \dot{Y}(0) = \bar{V}, \quad (\text{A.6})$$

where \bar{X} and \bar{Y} are the slip deficits of asperities 1 and 2, respectively, when the asperities start slipping together. Asperity 2, which was already slipping at the onset of mode 11, is associated with a certain rate \bar{V} , whereas asperity 1 is initially stationary. The slip deficits \bar{X} and \bar{Y} satisfy the Eq. (23) of Line 1. The constants are

$$A = \frac{1}{\omega_a} \left(\frac{\gamma}{2} B + \frac{\xi}{1 + \xi} \bar{V} \right), \quad (\text{A.7})$$

$$B = \frac{1}{1 + \xi} [\bar{X} + \xi \bar{Y} - \epsilon (1 + \beta \xi)], \quad (\text{A.8})$$

$$C = \frac{1}{\omega_b} \left(\frac{\gamma}{2} D - \frac{\xi}{1 + \xi} \bar{V} \right), \quad (\text{A.9})$$

$$D = \frac{\xi}{1 + \xi} [\bar{X} - \bar{Y} - \epsilon (X_P - Y_P)]. \quad (\text{A.10})$$

A.3 Case 00 → 11

The initial conditions are

$$X(0) = X_P, \quad Y(0) = Y_P, \quad \dot{X}(0) = 0, \quad \dot{Y}(0) = 0, \quad (\text{A.11})$$

where it was taken into account that P is defined as the state of the fault that satisfies the conditions for the failure of asperities 1 and 2 at the same time. Both asperities are initially stationary and their velocities are null at the beginning of the seismic event. The constants are

$$A = \frac{\gamma}{2\omega_a} B, \quad (\text{A.12})$$

$$B = \frac{1}{1 + \xi} (1 - \epsilon) (1 + \beta\xi), \quad (\text{A.13})$$

$$C = \frac{\gamma}{2\omega_b} D, \quad (\text{A.14})$$

$$D = \frac{\xi}{1 + \xi} (1 - \epsilon) (X_P - Y_P). \quad (\text{A.15})$$

References

- Amendola A, Dragoni M (2013) Dynamics of a two-fault system with viscoelastic coupling. *Nonlinear Processes Geophys* 20:1–10. <https://doi.org/10.5194/npg-20-1-2013>
- Chen T, Lapusta N (2009) Scaling of small repeating earthquakes explained by interaction of seismic and aseismic slip in a rate and state fault model. *J Geophys Res* 114:B01311. <https://doi.org/10.1029/2008JB005749>
- Di Bernardo M, Budd CJ, Champneys AR, Kowalczyk P (2008) *Piecewise-smooth dynamical systems: theory and applications*. Springer, Berlin
- Dragoni M, Lorenzano E (2015) Stress states and moment rates of a two-asperity fault in the presence of viscoelastic relaxation. *Nonlinear Processes Geophys* 22:349–359. <https://doi.org/10.5194/npg-22-349-2015>
- Dragoni M, Lorenzano E (2017) Dynamics of a fault model with two mechanically different regions. *Earth Planets Sp* 69:145. <https://doi.org/10.1186/s40623-017-0731-2>
- Dragoni M, Piombo A (2015) Effect of stress perturbations on the dynamics of a complex fault. *Pure Appl Geophys* 172(10):2571–2583. <https://doi.org/10.1007/s00024-015-1046-5>
- Dragoni M, Santini S (2012) Long-term dynamics of a fault with two asperities of different strengths. *Geophys J Int* 191:1457–1467. <https://doi.org/10.1111/j.1365-246X.2012.05701.x>
- Dragoni M, Santini S (2014) Source functions of a two-asperity fault model. *Geophys J Int* 196:1803–1812. <https://doi.org/10.1093/gji/ggt491>
- Dragoni M, Santini S (2015) A two-asperity fault model with wave radiation. *Phys Earth Planet Inter* 248:83–93
- Dragoni M, Tallarico A (2016) Complex events in a fault model with interacting asperities. *Phys Earth Planet Inter* 257:115–127
- Huang J, Turcotte DL (1990) Are earthquakes an example of deterministic chaos? *Geophys Res Lett* 17:223–226
- Jaeger JC, Cook NGW (1976) *Fundamentals of rock mechanics*. Chapman & Hall, London
- Lay T, Kanamori H, Ruff L (1982) The asperity model and the nature of large subduction zone earthquakes. *Earthq Pred Res* 1:3–71
- Lay T, Ammon CJ, Hutko AR, Kanamori H (2010) Effects of kinematic constraints on teleseismic finite-source rupture inversions: great Peruvian earthquakes of 23 June 2001 and 15 August 2007. *Bull Seismol Soc Am* 100(3):969–994
- Luo Y, Ampuero JP (2017) Stability of faults with heterogeneous friction properties and effective normal stress. *Tectonophysics*. <https://doi.org/10.1016/j.tecto.2017.11.006>
- McCloskey J, Bean CJ (1992) Time and magnitude predictions in shocks due to chaotic fault interactions. *Geophys Res Lett* 19:119–122
- Nussbaum J, Ruina A (1987) A two degree-of-freedom earthquake model with static/dynamic friction. *Pure Appl Geophys* 125:629–656
- Rice JR (1993) Spatio-temporal complexity of slip on a fault. *J Geophys Res* 98:9885–9907
- Ruff LJ (1983) Fault asperities inferred from seismic body waves. In: Kanamori H, Boschi E (eds) *Earthquakes: observation, theory and interpretation*. North-Holland, Amsterdam, pp 251–276
- Ruff LJ (1992) Asperity distributions and large earthquake occurrence in subduction zones. *Tectonophysics* 211:61–83
- Scholz CH (1990) *The mechanics of earthquakes and faulting*. Cambridge University Press, Cambridge

- Skarbak RM, Rempel AW, Schmidt DA (2012) Geologic heterogeneity can produce aseismic slip transients. *Geophys Res Lett*. <https://doi.org/10.1029/2012GL053762>
- Sladen A, Tavera H, Simons M, Avouac JP, Konca AO, Perfettini H, Audin L, Fielding EJ, Ortega F, Cavagnoud R (2010) Source model of the 2007 Mw 8.0 Pisco, Peru earthquake: implications for seismogenic behavior of subduction megathrusts. *J Geophys Res* 115(B2):2156–2202. <https://doi.org/10.1029/2009JB006429>
- Turcotte DL (1997) *Fractals and chaos in geology and geophysics*, 2nd edn. Cambridge University Press, Cambridge